Physicochemical assessment of atmospheric particulate matter emissions during open-pit mining operations in a massive sulphide ore exploitation

Carlos Boente[1,*], María Millán-Martínez[1], Ana M. Sánchez de la Campa[1], Daniel Sánchez-Rodas[1], Jesús D. de la Rosa[1]

[1] CIQSO-Center for Research in Sustainable Chemistry, Associate Unit CSIC-University of Huelva "Atmospheric Pollution", Campus El Carmen s/n, 21071 Huelva, Spain.

*Corresponding author: carlos.boente@dimme.uhu.es

Abstract

Mining operations are critical emission sources of atmospheric particulate matter (APM). This study constitutes a physicochemical characterisation of the main geochemical anomalies associated with APM by mining operations in the renowned Riotinto Mine (Iberian Pyrite Belt, Southwest Spain). The operations studied were traffic in the mining tracks, drilling, blasting, dry and wet loading of ore/waste, and stockpiling. Chemical analysis of PM_{10} and $PM_{2.5}$ comprised 46 potentially toxic elements (PTEs) and rare earth elements (REEs). The geochemical fingerprint of the operations in nearby populations was studied via environmental ratios after a comprehensive one-year sampling campaign at three monitoring stations. The results revealed that a notable amount of PM_{10} and $PM_{2.5}$ is released for the mining tracks, drilling, and dry loading. Moreover, enrichments of typical elements associated with sulphide ores (e.g. Cu, Ba, Zn, As, and Pb) were found, although some of them are also present in the APM geochemical background. These results are of substantial interest to air quality managers aiming to abate the main emission sources of APM and hazardous elements associated with mining processes.

Keywords: Atmospheric Particulate Matter; Toxic Elements; Mining; Massive sulphide ore.

Graphical abstract

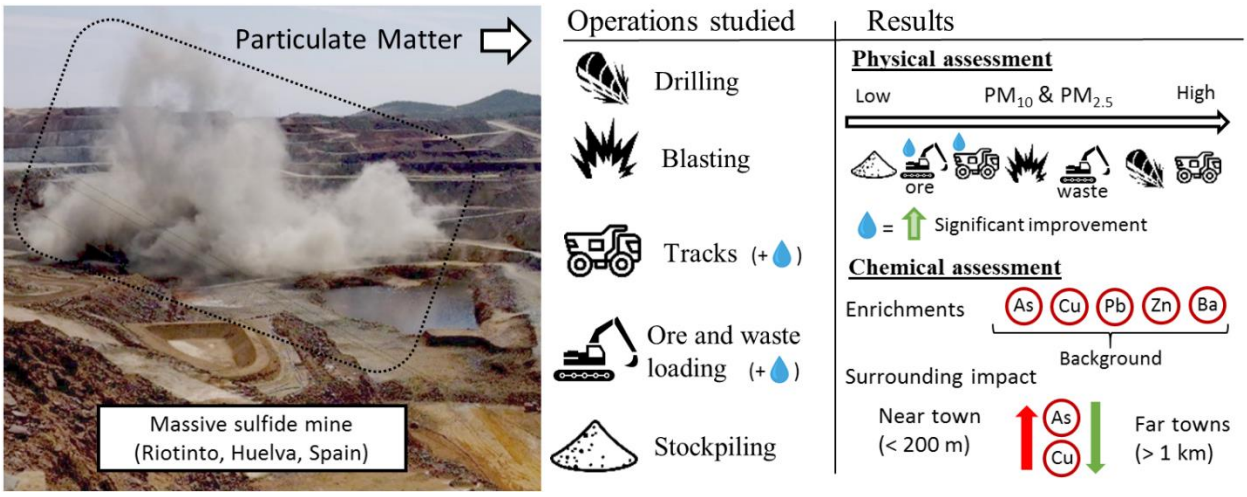

Highlights

- Dust emissions by mining operations in a massive sulphide mine were studied.
- Tracks, drilling, and dry loading are the main sources of particulate matter.
- A background of As, Ba, Cu, Pb, and Zn was identified in the particulate matter.
- Operations fingerprint on nearby towns was addressed through elemental ratios.

1. Introduction

The aerial transport of atmospheric particulate matter (APM) is one of the most important mechanisms of pollutant distribution over prolonged periods and at large spatial scales. The significant inhalation of APM may result in different health risks depending on their physical properties, namely particle size, shape, reactivity, solubility, and chemical composition (Nel, 2005; Plumlee and Ziegler, 2007). Physical characteristics involve lung cancer, silicosis, and other severe respiratory diseases (IARC, 1997). On the other hand, the chemical composition of APM is strongly related to the concentration of potentially toxic elements (PTEs) and rare earth elements (REEs). The capabilities of persistency and non-biodegradability of the PTEs and REEs result in rising bioaccumulation in the different environmental matrices, such as soils (Tóth et al., 2016;

Khanam et al., 2020), water (Pan and Wang, 2012; Vega et al., 2020), or sediments (Nawab et al., 2018; Eren et al., 2021), which, in the long run, may derive into health problems for the living organisms because of their high toxicity (Boreland and Lyle, 2006; Clemens, 2006; Liu and Liu, 2020).

Therefore, it is of vital importance to control and monitor pollution caused by APM emissions, and several studies have been conducted worldwide on this topic (Idris et al., 2020; Aguilera et al., 2021; Anwar et al., 2021; Millán et al., 2021). Mathematical models and tools, such as principal component analysis or positive matrix factorisation, have facilitated the identification and measurement of APM sources (Viana et al., 2008; Bove et al., 2014; Hopke, 2016; Feng et al., 2019). Some of them are natural, via resuspension of soils, sea salt aerosols, and desert dust (Middleton, 2017), while others have an anthropogenic origin, such as those related to traffic (Amato et al., 2009), industry (Cesari et al., 2014; Sánchez de la Campa et al., 2018), or biomass burning (Mieville et al., 2010).

Open-pit metallic mining is another unequivocal source of APM from multiple perspectives (Noble et al., 2016) that requires to forecast the air quality (Lu et al., 2021). It includes emissions originating from the extraction of metallic ore, mining heaps and associated leachates that affect soils and waters (El Khalil et al., 2008; Rieuwerts et al., 2014; Boente et al., 2019), acid mine drainage (Concas et al., 2006; Dold, 2014), or aerial dispersion attributable to grinding operations on in-mine mineral processing plants (Jankovic et al., 2000; Herbst et al., 2003; Lee et al., 2021). These operations release high amounts of APM, whose content in PTEs is excessive because of geological enrichment and may affect the environment, workers or residents near the mine (Csavina et al., 2012; Pandey et al., 2014). In this sense, some mining processes in combination with wind cause particulate suspension problems, such as: 1) rock drilling and subsequent blasting, which in addition to APM also emits toxic gases depending on the explosives (Zawadzka-Malota, 2015); 2) the loading, transport, and unloading of the ore and gangue; 3) oversized excavators, trucks, washers, and so forth, are frequently driven by diesel engines; or 4) stopped stockpiles during a prolonged time interval.

One of the most prolific opencast sulphide exploitations in Europe is Riotinto (Tornos, 2006; Martín-Crespo et al., 2011; Romero et al., 2015), in Huelva Province, southwest Spain. The mine ceased its processes in 2001 because of the low prices of Cu. In 2015,

operations were resumed with an increasing production, reaching 14.8 million tonnes of ore in 2019, with an average copper grade of 0.45% and a recovery rate of 84.53% (ATYM, 2021). Recently, a study revealed high concentrations of PTEs in the environment of the mine (Sánchez de la Campa et al., 2020). With these prospects, it is expected that the mining activities in this large district will last for several years. Hence, the importance of studying and controlling these APM emissions that, in other districts, have demonstrated that may cause harmful damage (Asif et al., 2018).

Thus, the objectives of this study are: 1) to assess the geochemical anomalies associated with APM produced in the Riotinto Mine and 2) identify those Cu-mining operations that are the most dangerous for the environment by quantifying the release of PTEs. This study considers fine (2.5 µm) and coarse (10 µm) APM particles ($PM_{2.5}$ and PM_{10}) produced by several mining operations and at different locations within the mine. For both particle sizes, 46 trace elements were chemically analysed, namely PTEs and REEs, and their enrichments were evaluated. Furthermore, APM collected at three monitoring stations in a surrounding town was also analysed during a full year; thus, the geochemical fingerprint of the mining operations can be evaluated. According to our review of the literature, this study provides one of the first assessments of APM produced during open-pit mining operations from a large massive sulphide active mine.

2. Materials and methods

2.1 Study area and mining operations producing APM

The Riotinto mining district (Huelva Province, Spain; Figure 1) belongs to the well-known Iberian Pyrite Belt-+. It is one of the largest massive polymetallic sulphides in the world (Leistel et al., 1997) and has been exploited since pre-Roman times (Davis Jr. et al., 2000). The main ore is pyrite (FeS_2), although chalcopyrite ($CuFeS_2$), arsenopyrite (FeAsS), galena (PbS), and sphalerite (ZnS) are also present. Another important mineral is gossan. In Riotinto, gossan had a dual function: a guide to buried ore deposits used by prospectors in their quest for the abovementioned metal sulphide ores, and being mined to obtain gold, silver and copper, this later the principal metal exploited in the area (Tornos, 2006).

A brief explanation of the opencast exploitation is as follows, according to Atalaya Mining (Atalaya Mining, 2021. Personal Communication) The mine has multiple haulage roads for traffic, which is essentially composed of dumper trucks, apart from other mining machinery (e.g. backhoes and drillers). The main access tracks are watered daily, whereas the tracks to the ponds are not. Regarding mining processes, perforation is performed through drilling carriages. Subsequently, blastings are conducted through pumped explosive emulsions, which, in addition to APM, cause the release of toxic gases (e.g. NO_2). The ore is backhoe-loaded in dumpers under wet conditions. Waste, whose content in PTEs is expected to be low, is loaded under dry conditions. The mineral is transported to the mineral processing plant and stored in stockpiles at certain stages. Processing methods comprise crushing, grinding, and flotation to obtain a Cu concentrate. More specifically, the crushed ore is reduced to 165 mm. The mineral is transferred to the coarse warehouse and then transported to the secondary and tertiary crushing circuits. This process is completed with a screening, obtaining a particle size of 16 mm to be stored in the 'fine warehouse'. Subsequently, a primary mill reduces the mineral to a final size of up to 1.5 mm, where it is subjected to hydrocycloning where the particles are classified by gravity: the finer sizes, obtained by the overflow, pass through the flotation area, and the coarser sizes are sent to additional stages of grinding. The result is fine dust <160 μm, which is water-moistened and pumped to the flotation area to recover the metals by means of physical-chemical processes (Sánchez de la Campa et al., 2020).

Control operations for air quality are linked to implementing emission abatement technologies for fugitive particles into the atmosphere. The main technology is the abovementioned irrigation, performed with $CaCO_3$-neutralised water from mining processes. In addition, regeneration and adaptation of tailings and planning of operations considering atmospheric dispersion models minimise the impact of APM on the surrounding populations.

2.2 Sampling campaign

An intensive APM sampling campaign was conducted between 19 and 21 September 2017. September was selected because of the near complete absence of rain during this

month. Thus, the dust is expected to reach annual maximums, and subsequently the major emission rates, being the affection to the environment high. The scope was to obtain data on the level of APM and its chemical composition during different mining operations, which are the main sources of fugitive particles to the atmosphere in the Riotinto mining district (Sánchez de la Campa et al., 2020). The sampling methodology was similar to that of Alastuey et al. (2006). The operations and the duration of the APM sampling (in parenthesis) were as follows: main access watered track (1 h), drilling (30 min), two similar blastings on different days: blasting A (25 min), blasting B (40 min), wet ore loading (1 h), dry waste loading (1 h), stockpile during dry unloading (1 h), stockpile stopped (1 h), and particulate suspension by the circulation of dumpers in the tailings pond dry track (40 min).

The location of these operations is shown in Figure 1. The footage of mining operations during the campaign is shown in Figure 2. As it can be seen, the location of the sampling equipment was next to the operations, attending to weather forecast (wind direction and wind speed). In the case of blastings, sampling equipment was place as close as possible to them, considering the safety protocol of the Riotinto mine and trying to avoid possible damage or destruction of the equipment due to shock waves or projectiles. Notwithstanding, weather forecast was taken into consideration in order to reach the cloud of dust.

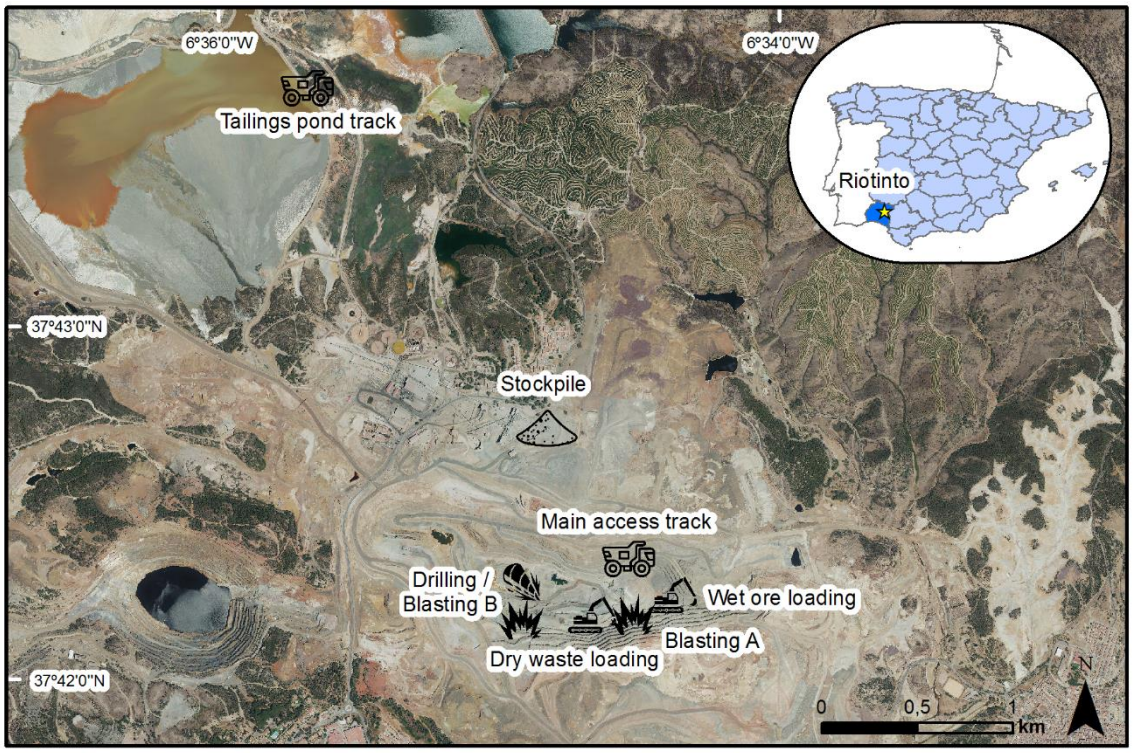

156

157 **Figure 1.** Location of monitoring stations for emission sources in the Riotinto Mine (Huelva, Spain) and
158 mining processes studied in each.

159

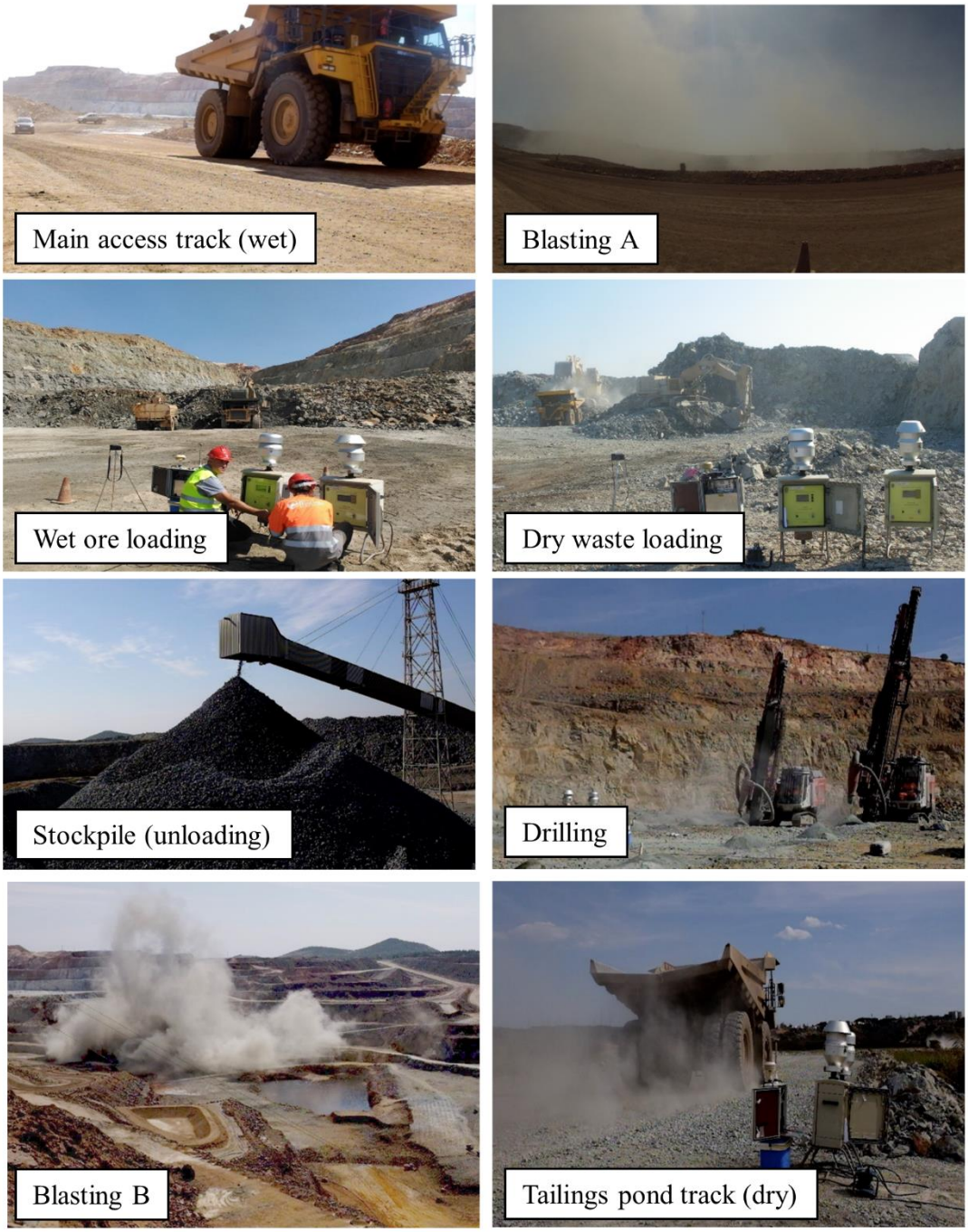

Figure 2. Visual release of dust during mining operations. Some photographs show the monitoring stations' equipment. Notable is the significance differences among the clouds of dust for the same operation (e.g. tracks, material loading) whether they are watered or not.

An online GRIMM 1107 optical counter was used to obtain the levels of total suspended particles (TSP), PM_{10} and $PM_{2.5}$ with one-minute resolution, in such a way the cyclic variations of the operations concerning PM were addressed. For a proper characterization of PM_{10} and $PM_{2.5}$, an additional sampling was performed using offline High Volume Air

Samplers (MCV CAV-A-PM1025, 30 m^3h^{-1}, standard procedure UNE-EN 12341, 2015). The inlets were equipped with PM_{10} and $PM_{2.5}$ Munktell® quartz fibre filters. For the blasts, the location of the samplers was established by considering the weather forecast and wind direction such that the dust cloud crossed the sampler. The activation in this case was automatic, reducing the time of analysis.

Additionally, to assess the fingerprint of the mining processes on the nearby populations of Nerva, Riotinto and La Dehesa, an air quality campaign was conducted from January to December 2018. Here, a daily sample every five days was collected using Munktell® PM_{10} quartz fibre filters using the same MCV CAV-A-PM1025 sampler.

2.3 Chemical analysis

All determinations were carried out following gravimetric standard procedure (UNE-EN 12341, 2015). Sampling filters were dried in a desiccator at 20 ºC during 24 h and 50% relative humidity, in accordance with standard procedures. Afterwards, they were weighed in a Sartorius LA 130 S-F balance, obtaining TSP, PM_{10} and $PM_{2.5}$ through gravimetric methods. In order to determine the chemical composition of this APM produced during the open pits, filters were subjected to analytical treatments following the methodology proposed by Querol et al. (2001). A half of each filter was subjected to acid digestion (2.5 mL HNO_3: 5 mL HF: 2.5 mL $HClO_4$). PTEs, REEs and other trace elements were quantified through ICP-MS (Agilent model 7900), using ^{103}Rh as internal standard to minimize the possible fluctuations of the plasma. For quality control, fly ash (NIST-1663b) was used as Reference Standard Material and analyzed in every analytical run. This provided values of accuracy and precision in the range of 5-10% for most elements studied.

2.4 Assessment of PTEs enrichment in particulate matter

For PM_{10}, enrichment factors (EFs) of PTEs in APM were calculated and compared with the geochemical background for air. EFs for an element (e) and a mining operation (MO) can be calculated by means of the following expression (Eq. 1) (Zoller et al., 1994):

$$EF_{e,MO} = \frac{\left[\frac{C_e}{C_{re}}\right]_{MO}}{\left[\frac{C_e}{C_{re}}\right]_{RB}} \quad (1),$$

where C_e is the concentration of an element 'e' in a mining operation 'MO' and in the selected reference background (RB). Similarly, C_{re} denotes the concentration of the reference element. For this study, scandium (Sc) was chosen as the reference element because among the elements identified as suitable for terrestrial studies (Reimann and de Caritat, 2005), Sc was present at suitable concentrations (e.g. between detection limits and not extremely high values) in the samples. For the RB sample, the mean concentrations of PM_{10} during the mine abandonment phase (2009–2014) were used, considering data from Sánchez de la Campa et al., 2020. The following classification is commonly used (Mummullage et al., 2016): EF values > 40 indicate extremely high enrichment, 20 < EF < 40 very high, 2 < EF < 20 significant, 2 < EF < 5 moderate, and EF < 2 minimal.

Additionally, the index of geoaccumulation (I_{geo}) was calculated to contrast the results and reinforce some hypotheses. Muller (1979) proposed the index of geoaccumulation for sediments, and it has also been applied in air pollution studies (Ali et al., 2017; Wei et al., 2015). I_{geo} is defined by Eq. 2:

$$I_{geo} = log_2\left(\frac{C_e}{1.5C_{e-RB}}\right) \quad (2),$$

where C_e is the concentration of the element 'e', and $C_{e\text{-}RB}$ is the concentration of the same element 'e' in the reference background sample, which is, again, the mean PM_{10} concentration during the abandonment phase (2009-2014). The classes of the I_{geo} are: unpolluted (I_{geo} < 1), poor pollution (1 < I_{geo} < 3), moderate pollution (3 < I_{geo} < 4), high pollution (4 < I_{geo} < 5), very high pollution (5 < I_{geo} < 6), and extreme pollution (I_{geo} > 6), which implies a 100-fold enrichment above the background.

Finally, data from the three monitoring stations near the towns of Riotinto, Nerva, and La Dehesa, corresponding to 2018, were compared with those from the MOs by using elemental ratios of mass concentrations. As suggested in the literature, we used ratios for

elements of interest such that the geochemical fingerprint of the operations is pursued (Mehra et al., 2020; Williamson et al., 2021). For this study, As, Cu, Pb, and Zn were selected as representative elements of concern in the APM samples.

3. Results and discussion

3.1 Levels of PM_{10} and $PM_{2.5}$

Concentrations of PM_{10} and $PM_{2.5}$ and information related to sampling time are shown in Table 1. Some differences can be observed in terms of operation. First, the process producing a maximum concentration of APM is the traffic in the dry track to the tailings pond (1587 $\mu g/m^3$ in PM_{10}, 929 $\mu g/m^3$ in $PM_{2.5}$). By contrast, the main access track, which was regularly watered, showed lower concentrations of PM_{10} (388 $\mu g/m^3$) and $PM_{2.5}$ (377 $\mu g/m^3$). This finding revealed the effectiveness of water irrigation. However, there are other possible solutions for APM abatement in dry region tracks such as Riotinto, for example, creating a film of impervious material to retain dust via Portland cement or bitumen from polymers or coal (Darling, 2011), as well as the use of novel suppressants that have already been effectively used in Cu-mines (Huang et al., 2019).

Drilling and blastings were also a notorious source of respirable dust in the Riotinto Mine. The former is commonly the mining operation causing a major amount of dust, as reported in the literature (Onder and Ygit, 2009), which is consistent with our results (787 $\mu gPM_{10}/m^3$ and 299 $\mu gPM_{2.5}/m^3$). Drilling is conducted by rotary percussive drilling rigs, carrying a rotary hammer that successively hits and fragments the rock, and the release of which is directly proportional to the drill hole diameter (Pandey, 2012). In this case, drilling was performed without dust depression systems. These high concentrations of APM could be reduced by up to three times under wet conditions, according to the literature (Bandopadhyay and Kumari, 2013). Additionally, blastings are controlled operations that result in concentrated clouds of dust with a high PM content. In this study, the two blastings analysed provided similar results (213 $\mu gPM_{10}/m^3$ and 289 $\mu gPM_{2.5}/m^3$ for blasting A and 307 $\mu gPM_{10}/m^3$ and 216 $\mu gPM_{2.5}/m^3$ for blasting B). These results are far below those obtained in blastings performed in other activities, such as building demolition (Wagner et al., 2017). Although these values could be reduced by applying strategies for the control of dust during blastings, as reviewed by Cecala et al. (2012), in

this case, we hypothesise that this reduction occurs because either the process of blasting is optimised to reduce the amount of dust, or the measurement devices (MCV/GRIMM) must be located further compared to other operations to avoid their destruction.

The immediate step after blasting is the damper loading of the material by means of a backhoe. In this regard, it was observed that dry waste loading is an operation with a high amount of dust release (690 $\mu gPM_{10}/m^3$ and 528 $\mu gPM_{2.5}/m^3$). In this context, the PM emitted during dry waste loading is more difficult to control because it depends largely on the ability of the backhoe operator while dropping material from height (Gustafson et al., 2017). However, as stated previously, the dust in this operation can be reduced by a factor of 3 if the material is previously watered (244 $\mu gPM_{10}/m^3$ and 143 $\mu gPM_{2.5}/m^3$, respectively).

Finally, the stockpile shows some of the lowest PM_{10} and $PM_{2.5}$ concentrations: 170 $\mu gPM_{10}/m^3$ and 154 $\mu gPM_{2.5}/m^3$ for the unloading, and 225 $\mu gPM_{10}/m^3$ and 262 $\mu gPM_{2.5}/m^3$ for the stopped stockpile. More specifically, in Riotinto Mine, unloading represents the least hazardous operation for PM concentration. Pollutant dispersion in a stockpile strongly depends on wind parameters, such as speed or direction (Badr and Harion, 2005). Owing to this dependency, locating an area of gentle winds to locate the stockpiles or to cover them is recommended. In this case, the mining company built a dome to avoid fugitive emissions (Atalaya Mining, 2021. Personal Communication) The dome is expected to produce a significant improvement in the management and control of this particulate matter source.

Table 1. Location, date, time, total volume (m^3), and mean concentrations of PM_{10} and $PM_{2.5}$ ($\mu g/m^3$) during measurement of levels and sampling in different sources (mining operations). Sampling campaign was carried out between 09/19/2017 and 09/21/2017.

	Sampling time			PM_{10}		$PM_{2.5}$	
Mining operation	**Start**	**End**	**Minutes**	**Sampling volume (m^3)**	**Conc. ($\mu g/m^3$)**	**Sampling Volume (m^3)**	**Conc. ($\mu g/m^3$)**
Main access track (wet)	12:20	13:20	60	30.9	388	30	377
Blasting A	13:30	13:54	24	12.2	213	12.1	289
Wet ore loading	15:45	16:50	65	32	244	30	143
Dry waste loading	10:33	11:31	58	28.7	690	28.2	528
Stockpile (stopped)	15:45	16:32	47	23.6	225	21.4	262
Stockpile (unloading)	10:46	11:47	61	30	170	29.9	154
Drilling	12:25	13:05	30	20.2	787	20.1	299
Blasting B	13:55	14:35	40	19.9	307	19.9	216
Tailings pond track (dry)	16:21	16:58	37	8	1587	7	929

As an approach to risk quantification, all the values substantially exceed the 24 h European Union limit values for PM_{10} (50 $\mu gPM_{10}/m^3$, Directive 2008/50/EC), from 3.4 times for the stockpile unloading, up to 31.7 times in the tailings pond track.

To rank the mining operations from least to most hazardous for the environment in the long term, their emission mechanisms and other parameters such as the frequency, the dust production and the dust resuspension have been assessed (Paluchamy et al. (2021). By considering this, the risk of the operations might be approximately hierarchised considering these variables together with results for PM_{10} and $PM_{2.5}$. All these features are presented in Table 2. Thus, attending to our results, the operations ordered from greater to lesser degree of risk are 1) haulage roads, 2) drilling, 3) dry loading, 4) blasting, and 5) stockpiling. At a more detailed level, regarding the most concerning operations, the tailings pond track, as a haulage road, is the most important source of dust in the

Riotinto Mine because of the continual traffic of mining vehicles. In this respect, because wetting all the tracks is unfeasible, it is of vital importance to reduce the dust produced by primary sources, because secondary sources thus also decrease (World Health Organization, 1999). Notably, we can posit that drilling might release large concentrations of PM_{10} and $PM_{2.5}$, but their contribution to the total dust level is small because this operation is rapidly performed and punctually produced in the mine (Mohamed et al., 1996).

Table 2. Dust sources in mining operations (adapted from Petavratzi et al., 2005 and references therein to the Riotinto case) and a comparison with results from Table 1.

Mining operation	Mechanism of emission	Frequency	Contribution to total dust levels	Dust production	Dust resuspension	Dust in Riotinto
Drilling	Air flush	Daily	Low	High	Low	High
Blasting	Air flush	Daily	Low	High	Low	Intermediate
Loading and dumping	Drop of material from height	Hourly	Moderate	Low	High	High (dry)
Mineral processing - Size reduction	Impact, abrasion and dropping from heights	Continually	High	High	Low	Not studied
Mineral processing - Concentration	Dry concentrators: Movement and friction	Continually	Low	High	Low	Not studied
Stockpiling	Wind blow, high wind speeds, dropping from height	Continually	Low	0	Low	Low
Haulage roads	Tyres, exhaust and cooling fans	Minutes	High	Low	High	Very high

Also notable is the online monitoring of APM with the GRIMM 1107 optical counter (Figure 3). This step is especially important for operations with a limited duration, such as drilling, blasting, or loading. The TSP values are included in Figure SM1. In Figure 3, the distribution of APM varies depending on the mining operations.

Episodic APM peak concentrations occurred in most of them. First, haulage roads (main access wet and tailing pond dry track) present peaks and zeros, indicating the clear influence of traffic. More specifically, the track to the tailings pond presents fine particles with higher mean concentrations of PM_{10} and $PM_{2.5}$, consistent with the results shown in Table 1. Drilling is a very stable operation whose main concern is limited to extreme concentration peaks of dust when the drilling machine is working. These outstanding

concentrations can be controlled by increasing watering. The reasons of the high stability of drilling are that the variables with high influence on dust production, namely drilling speed and rotational speed, can be easily controlled by the operators, as well as the fact that dust is produced by a single point/hole and not in large surfaces. Dry loading was the operation that saturated the GRIMM sensor the most, representing another operational concern. Nevertheless, wetting the material is a suitable solution because concentrations are highly reduced. In the blasting, the GRIMM optical counter receives few fine particles until minute 5, when the dust cloud arrives. Once the cloud passes, punctual wind-dependent peak concentrations are obtained. However, in general, a dilution of fine particles is appreciated. Last, the curves for the stockpile show appreciable peaks with punctual high values of fine particles when the stockpile is stopped, which are highly reduced when unloading operations occur in the stockpile. Although the values are not extremely high, that the stopped stockpile permanently release fugitive particles is a detail to consider and should be monitored.

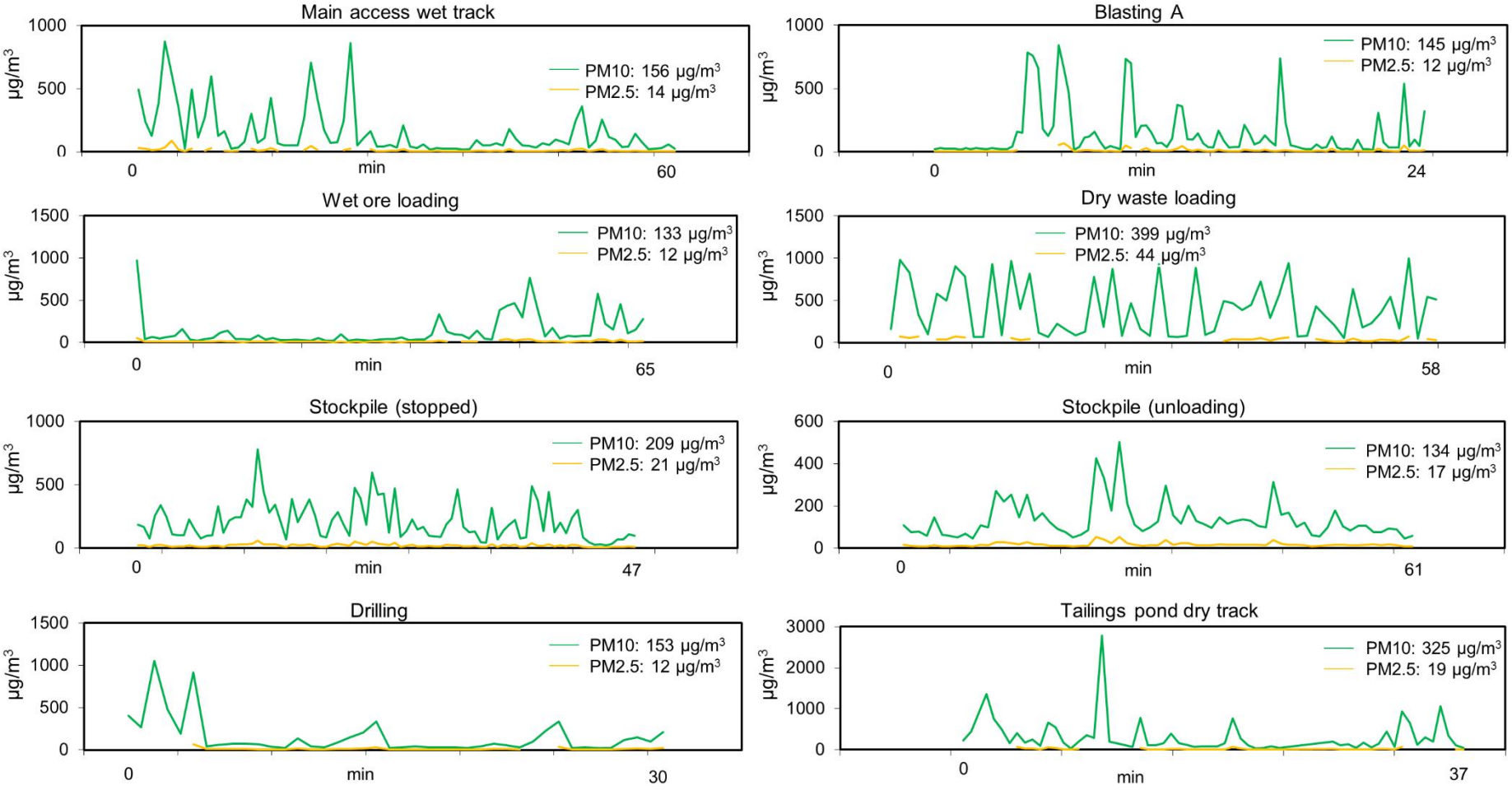

Figure 3. Time series of PM_{10} and $PM_{2.5}$ (µg/m^3) and mean values for different operations. Cuts in the $PM_{2.5}$ line represent values below detection limit.

3.2 Chemical composition of PM_{10} and $PM_{2.5}$

In addition to the identification of the main APM emission sources, the chemical composition of APM has been also study. To achieve this objective, the concentrations for main PTEs, minor elements and REEs analysed by ICP-MS in Table 3. Full data matrix can be found in Supplementary Materials section (Table SM1 for PTEs and Table SM2 for REEs).

According to the literature, the most significant PTEs of sulphide mineralisation in the Iberian Pyrite Belt are Cu, Pb, Zn, and As (Sáez et al., 1996; Tornos, 2006; Chopin and Alloway, 2007). The chemical analysis results (Table 3) reveal that these elements are enriched in the APM (e.g. PM_{10} maximums: 229.4 ngAs/m^3; 4842 ngCu/m^3; 555 ngPb/m^3; and 2382 ngZn/m^3), as well as Ba (PM10 maximum 3521 ngBa/m^3).

Although these values may seem high, they are considerably far from hazardous to the environment. In this context, the SME Mining Engineering Handbook (2011) presents permissible exposure limits (PELs) for exposure to metallic dust in mining (e.g. 0.15 mgPb/m^3, As 0.5 mgAs/m^3, 0.5 mgSb/m^3, 5 mgZn/m^3, or 0.5 mgV/m^3). Concerning the Spanish regulations, there is no specific standards for mining. However, for working environments there exist the Spanish occupational exposure limits (Spanish Ministry of Labour and Social Economy, 2021). Some of the most restricting values are As (0.01 mgAs/m^3), Cu (0.1 mgCu/m^3), Pb (0.15 mgPb/m^3) or Sb (0.5 mgSb/m^3), but the mining operations are far from reaching these values. Therefore, the degree of affection of these PTEs to the environment is negligible. A similar scenario occurs for the REEs, whose content is mainly below detection limits, except that some enrichments in light REEs are more associated with geology (La, Ce).

An explanation for these low values may be that nowadays the Riotinto Mine is processing minerals with very low ore grades (Cu grade 0.45%, ATYM, 2021). This metal content is in line with other currently working low-grade copper mines, such as the 0.43% Cu Zijinshan Mine in China (Chen et al., 2020) or the 0.99% Cu Pará State Mine in Brazil (Nascimento et al., 2019).

Another important result is that the minimum concentrations of PM_{10} for As (45.9 ng/m^3), Cu (456 ng/m^3), Pb (74 ng/m^3), and Zn (168 ng/m^3) were high. This fact implies a geochemical background of these PTEs in the air, which may be of concern in the long term. When the mine was abandoned (2009–2014), the concentrations of some elements in surrounding areas were As (1.12 ng/m^3), Cu (6.1 ng/m^3), and Pb (4.75 ng/m^3) (Sánchez de la Campa et al., 2020), a significant difference with respect to the mining operations.

Table 3. Concentration of minor elements, PTEs and REEs in APM determined by ICP-MS for the different open-pit mining operations. Units expressed in ng/m^3. Values below the detection limit are denoted as '< D.L.'.

Element	Main access wet track PM_{10}	Blasting A PM_{10}	Wet ore loading PM_{10}	Dry waste loading PM_{10}	Stockpile (stopped) PM_{10}	Stockpile (unloading) PM_{10}	Drilling PM_{10}	Blasting B PM_{10}	Tailings pond dry track PM_{10}
As	229	45.9	80.6	73.9	55.4	62.4	87.2	67.2	229
Ba	1206	5.10	132	1510	< D.L.	515	616	661	3251
Bi	12.1	3.20	7.60	7.70	3.80	3.30	4.20	6.20	19.4
Cd	2.50	1.20	1.00	9.40	1.10	1.20	1.70	1.40	9.70
Ce	10.6	12.1	11.5	70.1	8.10	11.4	66.8	14.4	153
Co	10.7	4.00	4.10	23.1	3.60	6.20	55.1	14.8	35.6
Cr	177	< D.L.	0.50	67.8	< D.L.	88.0	47.9	90.7	251
Cu	1048	498	588	757	456	726	2181	986	4842
La	4.40	6.40	6.40	32.4	4.20	5.20	31.7	6.50	74.0
Mo	943	< D.L.	23.8	129	< D.L.	186	5.80	160	744
Ni	631	< D.L.	< D.L.	148	< D.L.	161	155	213	552
Pb	458	74.8	158	145	158	120	86.7	92	555
Sb	54.0	13.2	27.2	23.7	15.4	20.0	13.7	17.7	65.5
Sn	17.1	6.40	6.70	35.7	7.70	14.6	13.0	7.40	81.8
V	10.6	4.60	4.40	15.4	6.10	5.30	17.4	14.0	32.6
Zn	1280	383	309	874	168	624	1719	789	2382

3.3 Enrichments of PTEs

To identify the degree of enrichment of the elements produced in the mining operations, EFs were calculated on the basis of the mean PM_{10} concentration when the mine was abandoned (2009–2014), using Sc as the reference element. The PTEs studied were those presenting high and variable concentrations among operations: As, Ba, Cr, Cu, Mo, Ni, Pb, and Zn (Figure 4a). For $PM_{2.5}$, EFs were not calculated, because some operations presented many values below the detection limits.

Regarding PTEs, the most concerning is Cu, which appears highly enriched in all operations, except dry waste loading, followed by As (arsenopyrite), with high enrichment in the wet loading of ore and stockpiles. Cu and Pb, despite being a notable part of the mineral phase (sphalerite and galena, respectively) did not appear highly enriched. Regarding the operations, the main access track is the chief concern, presenting significant enrichment ($2 < EF < 20$) for all PTEs, especially As, Cu, Mo, and Ni.

The case of high enrichment of Ni and other metals in the main access track is attributable to the fact that the main tracks are large and located in the exploitation area. Subsequently, they are permanently exposed to the deposition of elements coming from the mineralization and all the other mining operations, causing accumulation of metals over

time. On the one hand, metals in the loadings are exclusively affected by the own nature of the operation. Thus, loading of waste material, although being performed under dry conditions, contain lower concentration of metals. On the other hand, the loading of the ore, which would contain a higher concentration of Cu, As, Pb etc., is carried out under wet conditions (irrigation) so the major part is deposited in the soil.

Notably, throughout this research, high amounts of dust with a high content of PTEs are present in the tailings pond track or during the dry loading of waste (e.g. 229 ng/m^3 of As or 757 ng/m^3 of Cu, respectively), while the EFs reveal low enrichment for all PTEs. This result is a limitation of EFs which occurs because, according to the results in Tables 3 and 4, the majority of the elements in some operations surpass the remaining operations in one or more orders of magnitude, and choosing an element of reference that is not excessively enriched is difficult. To solve this problem, we contrasted these results with the Igeo (Figure 4b), which is not vitiated by this circumstance, because it does not use a specific element of reference and only compares the concentration of the element with the RB.

The visualisation of Igeo demonstrates that the threshold of high pollution (Igeo > 4) is practically exceeded for all elements and mining operations. This result is especially relevant in PTEs native to mineralisation: Cu, Zn, and Ba, as the main elements, and Pb and As to a minor extent, which are common elements in sulphide materials (Bouse et al., 1999). Regarding the operations, the tailings pond dry track is the only operation presenting three elements above Igeo > 14 (Ba, Cu, and Zn). The next operations are the main access wet track (again, Ba, Cu, and Zn, with Igeo > 12), drilling (Ba, Cu, and Zn, with Igeo > 12), and dry waste loading (Ba and Zn, with Igeo > 12), which is consistent with the results presented in prior sections. This phenomenon indicates that these operations are the most concerning from both the physical and chemical perspectives.

High enrichments for the aforementioned elements are expected because the mine is working with pure sulphide mineralisation, as evidenced in the literature (Csavina et al., 2014). Regarding the effect on other environmental matrices, a recent study of soils in the Riotinto area declared that these are not hazardous to humans (Romero-Baena et al., 2021), and another study reported that the hazard index for soils and groundwater was within an acceptable risk level (Rivera et al., 2016). Regarding air pollution, some studies

have revealed low effects outside the mining domain (Sánchez de la Campa et al., 2020). In this context, water and soil are more stable and invariant to pollution than air. Thus, based on the low concentrations we found in the sources in this study, our conclusion is that the mining operations do not have a deep impact on the surrounding environmental matrices from a chemical perspective.

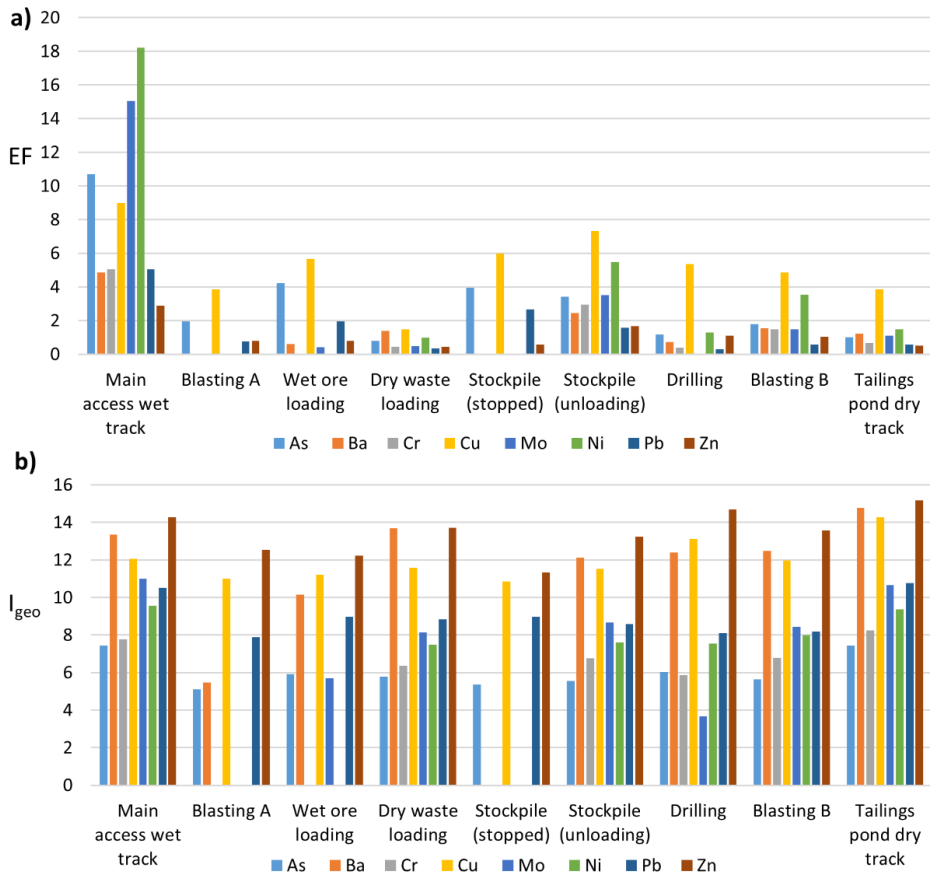

Figure 4. For the mining operations and concerning elements: a) Enrichment factors (EFs); b) Index of geoaccumulation.

3.4 Elemental ratios: air quality assessment in surrounding urban areas

During 2018, the air quality at three stations in surrounding urban areas between 0–2 km from the operations (Nerva, Riotinto, and La Dehesa; Figure 5) was monitored. Elemental ratios were calculated for some of the concerning pollutants and related to geochemical

anomalies of sulphide highlighted in Section 3.2 (Cu, As, Zn, and Pb). By means of elemental ratios we could combine the annual mean concentration of PM_{10} for different PTEs obtained at these urban stations (Table 4) and those corresponding to mining operations (Table 3). This comparison of patterns enabled us to rank the operations by their degree of impact on urban areas and follow the fingerprints of the operations (Figure 5).

In Table 4, the monitoring station in the town of La Dehesa, which is the closest to the mine, presented the highest mean concentration of pollutants during 2018. In this case, the As concentration in PM_{10} is near the objective limit of this pollutant (6 ng/m^3, 2008/50/EC). In descending hazard, Riotinto and Nerva PM_{10} contain between 2 and 4 times lower concentrations of PTEs than La Dehesa, revealing lower pollution.

Table 4. Mean concentrations of PTEs (ng/m^3) in three monitoring stations at surrounding populations during 2018. Mean concentrations of other elements can be consulted in Supplementary Materials section (Table SM3).

Element	Nerva	Riotinto	La Dehesa
As	1.83	1.80	5.88
Cu	15.4	22.5	98.3
Pb	5.73	5.98	14.9
Zn	27.7	25.8	43.7

On this basis, some patterns can be observed in Figure 5. Both operations and monitoring stations were classified into two clusters. First, Cluster 1 contained the majority of operations. All of them are very close to each other in terms of distance ratios, and they are related to those of the less affected stations of Nerva and Riotinto. The presence in this cluster of the main access wet track is highlighted. Cluster 2 contains La Dehesa and three mining operations, the most concerning are the tailings pond track (dry track) and the stockpile stopped, which is very close in distance; the wet ore loading was slightly more separated. In this regard, during the unloading in the stockpile, the values are more similar to those of Nerva despite the distance, which are the same as those for La Dehesa. This result suggests low affection during the unloading, but unfortunately, this is a punctual operation; therefore, measures are required to control the stockpiles when they are stopped to avoid affection at short distances (La Dehesa). For the tailings pond dry track, it was confirmed again that this operation is the most dangerous, evidencing the importance of proper wetting of the tracks to avoid dust scattering.

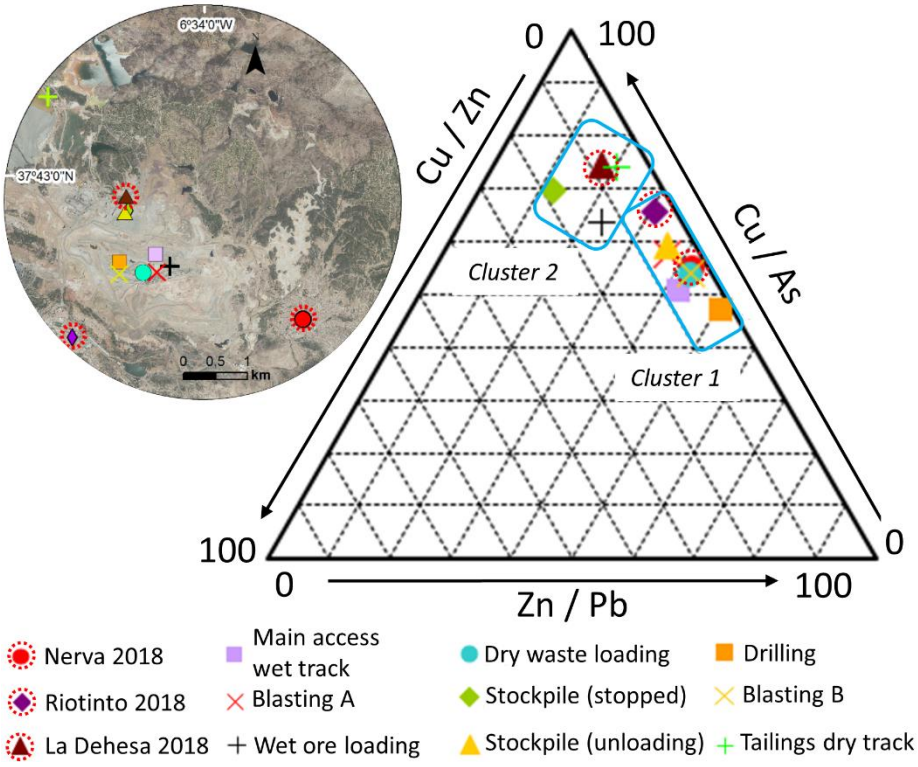

454

455 **Figure 5.** Triangular diagram showing elemental ratios for PTEs (PM_{10}) of concern for the three
456 monitoring stations (mean form all filters 2018, red-circled) and the mining operations. Main clusters are
457 blue-circled. On the left is the location of the points of study.

458 These clusters can also be clearly identified when plotting all the filter analyses and the
459 operations in a double-variable diagram Cu/Zn x-axis versus Zn/(10*As) y-axis (Figure
460 6). In this case, it can be observed that samples from La Dehesa and all mining operations
461 are very close to zero on the y-axis. This confirms a higher enrichment of As with respect
462 to the samples of Nerva and Riotinto, which have higher variability on the y-axis. The
463 distinction between monitoring stations is also visible in the x-axis: as La Dehesa samples
464 and operations from the concerning cluster (Cluster 2), attending to the high values of
465 Cu/Zn ratio, are clearly enriched in Cu, the principal element that is exploited in this
466 massive sulphide deposit. This allows to conclude that there is a high enrichment of
467 pollutants related to massive sulphide ore near the mine (La Dehesa station and the mining
468 operations), but not in the other two towns that are far from the mine, due to an intense
469 dilution effect.

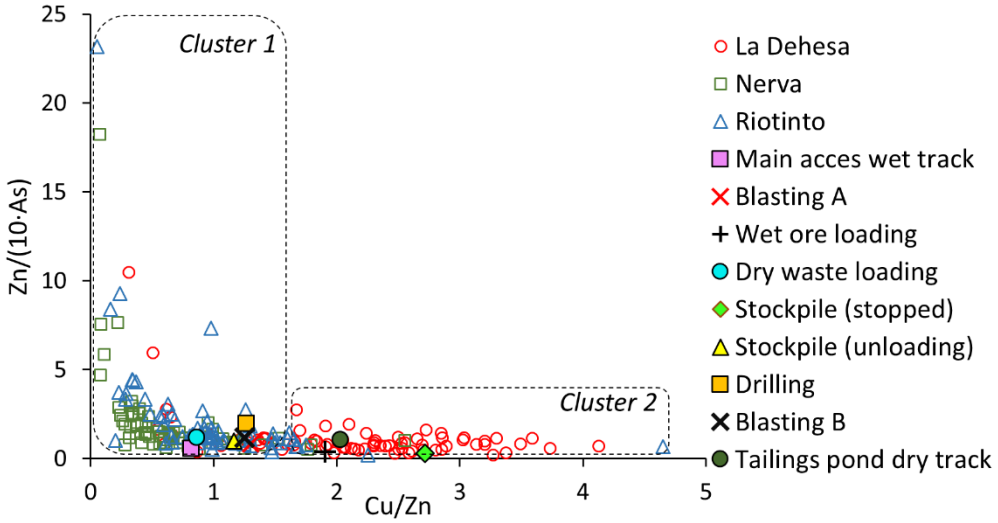

Figure 6. Selected ratios and point cloud for all filters studied in the three monitoring stations and mining operations.

4. Conclusion

This work corresponds to one of the first physicochemical assessments of APM originated by mining operations of a large sulphide exploitation. All the operations studied (traffic tracks, loading of ore and waste, drilling, blasting, and stockpiling) produced high concentrations of PM_{10} and $PM_{2.5}$. Moreover, it has proved that wetting the material through irrigation significantly abates the amount of APM in the air. In this context, $CaCO_3$-water irrigation is recommended for ore materials and waste. However, APM affects the entire mine. To evaluate the APM distribution, we highly recommend the use of low-cost sensors for monitoring APM in real time.

Regarding the content of PTEs in APM, enrichments were found for Cu, Ba, Zn, As, and Pb, with practically no presence of REEs, which is consistent with the geology of massive sulphide deposits. The operations with the highest concentrations of PTEs were also tracks, dry loading, and drilling. However, the concentrations were far from the PEL values, which may explain the low effect on the environmental matrices reported by other authors.

To assess the geochemical fingerprint of these APMs in the long term, the evolution of PM_{10} was monitored throughout 2018 at three stations located in surrounding populations.

The pattern of La Dehesa, the nearest town to the mine, is very similar to the most concerning operation, which correspond to the tailings pond dry track, the stockpile, and the ore loading, despite being performed under wet conditions. Other nearby towns, Nerva and Riotinto, show very similar patterns to the rest of the less hazardous or distant operations with a low enrichment in the main pollutants, Cu and As. The results of this study can help air quality managers to understand the geochemical anomalies of APM emitted by several mining operations occurring in massive sulphide mines.

CRediT author statement

Carlos Boente: Data Curation, Formal Analysis, Writing - Original Draft, Visualization. **María Millán**: Investigation, Resources. **Ana Sánchez de la Campa**: Methodology, Investigation, Writing - Review & Editing, Supervision. **Daniel Sánchez Rodas**: Writing - Review & Editing, Supervision. **Jesús D. De la Rosa**: Methodology, Data Curation, Writing - Review & Editing, Supervision, Project Administration, Funding Acquisition.

Declaration of competing interest

The authors declare that they have no known competing financial interests or personal relationships that could have appeared to influence the work reported in this paper.

Acknowledgements

Authors are grateful to Atalaya Mining Company for its permission to carry out this research on their facilities and to its active support. Carlos Boente obtained a post-doctoral contract within the program PAIDI 2020 (Ref 707 DOC 01097) and PY18-2332 Project, co-financed by the Junta de Andalucía (Andalusian Government) and the EU.

References

Aguilera, A., Bautista, F., Gutiérrez-Ruiz, M., Ceniceros-Gómez, A.E., Cejudo, R., Goguitchaichvili, A., 2021. Heavy metal pollution of street dust in the largest city of Mexico, sources and health risk assessment. Environ. Monit. Assess. 193, 193. doi:10.1007/s10661-021-08993-4

Alastuey, A., Ruiz, C., Sánchez de la Campa, A., de la Rosa, J.D., Mantilla, E., García dos Santos, S. Identification and Chemical Characterization of Industrial Particulate Matter Sources in Southwest Spain. J. Air & Waste Manage. Assoc. 56, 993-1006. doi: 10.1080/10473289.2006.10464502.

Ali, M.U., Liu, G., Yousaf, B., Abbas, Q., Ullah, H., Munir, M.A.M., Fu, B., 2017. Pollution characteristics and human health risks of potentially (eco)toxic elements (PTEs) in road dust from metropolitan area of Hefei, China. Chemosphere 181, 111–121. doi:10.1016/j.chemosphere.2017.04.061

Amato, F., Pandolfi, M., Escrig, A., Querol, X., Alastuey, A., Pey, J., Perez, N., Hopke, P.K., 2009. Quantifying road dust resuspension in urban environment by Multilinear Engine: A comparison with PMF2. Atmos. Environ. 43, 2770–2780. doi:10.1016/j.atmosenv.2009.02.039

Anwar, M.N., Shabbir, M., Tahir, E., Iftikhar, M., Saif, H., Tahir, A., Murtaza, M.A., Khokhar, M.F., Rehan, M., Aghbashlo, M., Tabatabaei, M., Nizami, A.-S., 2021. Emerging challenges of air pollution and particulate matter in China, India, and Pakistan and mitigating solutions. J. Hazard. Mater. 416, 125851. doi:10.1016/j.jhazmat.2021.125851

Asif, Z., Chen, Z., Guo, J., 2018. A study of meteorological effects on PM2.5 concentration in mining area. Atmos. Pollut. Res. 9, 688–696. doi:10.1016/j.apr.2018.01.004

ATYM., 2021. Consolidated and Company financial assessments, pp. 4.

Badr, T., Harion, J.L., 2005. Numerical modelling of flow over stockpiles: Implications on dust emissions. Atmos. Environ. 39, 5576–5584. doi:10.1016/j.atmosenv.2005.05.053

Boente, C., Albuquerque, M.T.D., Gerassis, S., Rodríguez-Valdés, E., Gallego, J.R., 2019. A coupled multivariate statistics, geostatistical and machine-learning approach to address soil pollution in a prototypical Hg-mining site in a natural reserve. Chemosphere 218, 767–777. doi:10.1016/j.chemosphere.2018.11.172

543 Boreland, F., Lyle, D.M., 2006. Lead dust in Broken Hill homes: Effect of remediation
544 on indoor lead levels. Environ. Res. 100, 276–283. doi:10.1016/j.envres.2005.06.007

545 Bouse, R.M., Ruiz, J., Titley, S.R., Tosdal, R.M., Wooden, J.L., 1999. Lead isotope
546 compositions of Late Cretaceous and early Tertiary igneous rocks and sulfide minerals in
547 Arizona; implications for the sources of plutons and metals in porphyry copper deposits.
548 Econ. Geol. 94, 211–244. doi:10.2113/gsecongeo.94.2.211

549 Bove, M.C., Brotto, P., Cassola, F., Cuccia, E., Massabò, D., Mazzino, A., Piazzalunga,
550 A., Prati, P., 2014. An integrated PM2.5 source apportionment study: Positive Matrix
551 Factorisation vs. the chemical transport model CAMx. Atmos. Environ. 94, 274–286.
552 doi:10.1016/j.atmosenv.2014.05.039

553 Cecala, A.B., O'Brien, A.D., Schall, J., Colinet, J.F., Fox, W.R., Franta, R.J., Joy, J.,
554 Reed, W.R., Reeser, P.W., Rounds, J.R., Schultz, M.J. 2012. Dust control handbook for
555 industrial minerals mining and processing. Report of investigations 9689, National
556 Institute for Occupational Safety and Health

557 Cesari, D., Genga, A., Ielpo, P., Siciliano, M., Mascolo, G., Grasso, F.M., Contini, D.,
558 2014. Source apportionment of PM 2.5 in the harbour–industrial area of Brindisi (Italy):
559 Identification and estimation of the contribution of in-port ship emissions. Sci. Total
560 Environ. 497–498, 392–400. doi:10.1016/j.scitotenv.2014.08.007

561 Chen, J., Zhong, S., Tang, D., Kuang, C., 2020. Practical Experience in Large-Scale
562 Development of Zijinshan Low-Grade Gold-Copper Mine. Mining, Metall. Explor. 37,
563 1339–1347. doi:10.1007/s42461-020-00237-2

564 Chopin, E.I.B., Alloway, B.J., 2007. Trace element partitioning and soil particle
565 characterisation around mining and smelting areas at Tharsis, Ríotinto and Huelva, SW
566 Spain. Sci. Total Environ. 373, 488–500. doi:10.1016/j.scitotenv.2006.11.037

567 Clemens, S., 2006. Toxic metal accumulation, responses to exposure and mechanisms of
568 tolerance in plants. Biochimie 88, 1707–1719. doi:10.1016/j.biochi.2006.07.003

569 Concas, A., Ardau, C., Cristini, A., Zuddas, P., Cao, G., 2006. Mobility of heavy metals
570 from tailings to stream waters in a mining activity contaminated site. Chemosphere 63,
571 244–253. doi:10.1016/j.chemosphere.2005.08.024

572 Csavina, J., Field, J., Taylor, M.P., Gao, S., Landázuri, A., Betterton, E.A., Sáez, A.E.,
573 2012. A review on the importance of metals and metalloids in atmospheric dust and
574 aerosol from mining operations. Sci. Total Environ. 433, 58–73.
575 doi:10.1016/j.scitotenv.2012.06.013

576 Csavina, J., Taylor, M.P., Félix, O., Rine, K.P., Eduardo Sáez, A., Betterton, E.A., 2014.
577 Size-resolved dust and aerosol contaminants associated with copper and lead smelting
578 emissions: Implications for emission management and human health. Sci. Total Environ.
579 493, 750–756. doi:10.1016/j.scitotenv.2014.06.031

580 Darling, P., 2011. SME Mining Engineering Handbook. Englewood, Colo.: Society for
581 Mining, Metallurgy, and Exploration.

582 Davis Jr., R.A., Welty, A.T., Borrego, J., Morales, J.A., Pendon, J.G., Ryan, J.G., 2000.
583 Rio Tinto estuary (Spain): 5000 years of pollution. Environ. Geol. 39, 1107–1116.
584 doi:10.1007/s002549900096

585 Directive 2008/50/EC of the European Parliament and of the Council of 21 May 2008 on
586 ambient air quality and cleaner air for Europe

587 Dold, B., 2014. Evolution of Acid Mine Drainage Formation in Sulphidic Mine Tailings.
588 Minerals 4, 621–641. doi:10.3390/min4030621

589 El Khalil, H., El Hamiani, O., Bitton, G., Ouazzani, N., Boularbah, A., 2008. Heavy metal
590 contamination from mining sites in South Morocco: Monitoring metal content and
591 toxicity of soil runoff and groundwater. Environ. Monit. Assess. 136, 147–160.
592 doi:10.1007/s10661-007-9671-9

593 Eren, S.T., Sungur, A., Ekinci, H., 2021. Trace metal fractions, sources, and risk
594 assessment in sediments from Umurbey Stream (Çanakkale-Turkey). Environ. Monit.
595 Assess. 193, 347. doi:10.1007/s10661-021-09134-7

596 Feng, W., Guo, Z., Peng, C., Xiao, X., Shi, L., Zeng, P., Ran, H., Xue, Q., 2019.
597 Atmospheric bulk deposition of heavy metal(loid)s in central south China: Fluxes,
598 influencing factors and implication for paddy soils. J. Hazard. Mater. 371, 634–642.
599 doi:10.1016/j.jhazmat.2019.02.090

600 Gustafson, A., Paraszczak, J., Tuleau, J., Schunnesson, H., 2017. Impact of technical and
601 operational factors on effectiveness of automatic load-haul-dump machines. Trans.
602 Institutions Min. Metall. Sect. A Min. Technol. 126, 185–190.
603 doi:10.1080/14749009.2017.1285980

604 Herbst, J.A., Yi, C.L., Flintoff, B., 2003. Size reduction and liberation. In: Fuerstenau,
605 M.C., Han, K.N., (Eds.) Principals of mineral processing. SME, Colorado, pp 69–95

606 Hopke, P.K., 2016. Review of receptor modeling methods for source apportionment. J.
607 Air Waste Manage. Assoc. 66, 237–259. doi:10.1080/10962247.2016.1140693

608 Huang, Z., Zhang, L., Yang, Z., Zhang, J., Gao, Y., Zhang, Y., 2019. Preparation and
609 properties of a rock dust suppressant for a copper mine. Atmos. Pollut. Res. 10, 2010–
610 2017. doi:10.1016/j.apr.2019.09.008

611 IARC., 1997 International Agency for Research on Cancer. Silica. IARC Monograph 68
612 on the Evaluation of the carcinogenic risk of chemicals to humans

613 Idris, S.A. "Ainaa," Hanafiah, M.M., Khan, M.F., Hamid, H.H.A., 2020. Indoor
614 generated PM2.5 compositions and volatile organic compounds: Potential sources and
615 health risk implications. Chemosphere 255, 126932.
616 doi:10.1016/j.chemosphere.2020.126932

617 Jankovic, A., Valery, W., La Rosa, D., 2000. Fine grinding in Australian mineral industry.
618 J. Min. Metall. A. 36, 51–61.

619 Khanam, R., Kumar, A., Nayak, A.K., Shahid, M., Tripathi, R., Vijayakumar, S., Bhaduri,
620 D., Kumar, U., Mohanty, S., Panneerselvam, P., Chatterjee, D., Satapathy, B.S., Pathak,
621 H., 2020. Metal(loid)s (As, Hg, Se, Pb and Cd) in paddy soil: Bioavailability and potential

risk to human health. Sci. Total Environ. 699, 134330. doi:10.1016/j.scitotenv.2019.134330

Kumar Bandopadhyay, A., Kumari, S., 2013. Quartz in Respirable Airborne Dust in Workplaces in Selected Coal and Metal Mines in India, in: Silica and Associated Respirable Mineral Particles. ASTM International, 100 Barr Harbor Drive, PO Box C700, West Conshohocken, PA 19428-2959, pp. 28–38. doi:10.1520/STP156520120125

Lee, P.-K., Lim, J., Jeong, Y.-J., Hwang, S., Lee, J.-Y., Choi, B.-Y., 2021. Recent pollution and source identification of metal(loid)s in a sediment core from Gunsan Reservoir, South Korea. J. Hazard. Mater. 416, 126204. doi:10.1016/j.jhazmat.2021.126204

Leistel, J.M., Marcoux, E., Thiéblemont, D., Quesada, C., Sánchez, A., Almodóvar, G.R., Pascual, E., Sáez, R., 1997. The volcanic-hosted massive sulphide deposits of the Iberian Pyrite Belt. Miner. Depos. 33, 2–30. doi:10.1007/s001260050130

Liu, T., Liu, S., 2020. The impacts of coal dust on miners' health: A review. Environ. Res. 190, 109849. doi:10.1016/j.envres.2020.109849

Lu, X., Zhou, W., Qi, C., Luo, H., Zhang, D., Pham, B.T., 2021. Prediction into the future: A novel intelligent approach for PM2.5 forecasting in the ambient air of open-pit mining. Atmos. Pollut. Res. 12, 101084. doi:10.1016/j.apr.2021.101084

Martín-Crespo, T., Martín-Velázquez, S., Gómez-Ortiz, D., De Ignacio-San José, C., Lillo-Ramos, J., 2011. A Geochemical and Geophysical Characterization of Sulfide Mine Ponds at the Iberian Pyrite Belt (Spain). Water, Air, Soil Pollut. 217, 387–405. doi:10.1007/s11270-010-0595-6

Mehra, M., Zirzow, F., Ram, K., Norra, S., 2020. Geochemistry of PM2.5 aerosols at an urban site, Varanasi, in the Eastern Indo-Gangetic Plain during pre-monsoon season. Atmos. Res. 234, 104734. doi:10.1016/j.atmosres.2019.104734

Middleton, N.J., 2017. Desert dust hazards: A global review. Aeolian Res. 24, 53–63. doi:10.1016/j.aeolia.2016.12.001

649 Mieville, A., Granier, C., Liousse, C., Guillaume, B., Mouillot, F., Lamarque, J.-F.,
650 Grégoire, J.-M., Pétron, G., 2010. Emissions of gases and particles from biomass burning
651 during the 20th century using satellite data and an historical reconstruction. Atmos.
652 Environ. 44, 1469–1477. doi:10.1016/j.atmosenv.2010.01.011

653 Millán-Martínez, M., Sánchez-Rodas, D., Sánchez de la Campa, A.M., Alastuey, A.,
654 Querol, X., de la Rosa, J.D., 2021. Source contribution and origin of PM10 and arsenic
655 in a complex industrial region (Huelva, SW Spain). Environ. Pollut. 274, 116268.
656 doi:10.1016/j.envpol.2020.116268

657 Ministry of Labour and Social Economy, 2021. Spanish occupational exposure limits.

658 Mohamed, M A.K., Mutmansky, J M, and Jankowski, R A., 1996. Overview of proven
659 low cost and high efficiency dust control strategies for mining operations. United
660 Kingdom.

661 Müller, G. (1979) Schwermetalle in den sediments des Rheins-Veranderungenseitt 1971.
662 Umschan, 79, 778-783.

663 Mummullage, S., Egodawatta, P., Ayoko, G.A., Goonetilleke, A., 2016. Use of
664 physicochemical signatures to assess the sources of metals in urban road dust. Sci. Total
665 Environ. 541, 1303–1309. doi:10.1016/j.scitotenv.2015.10.032

666 Nascimento, D., Lucheta, A., Palmieri, M., Carmo, A., Silva, P., Ferreira, R., Junca, E.,
667 Grillo, F., Alves, J., 2019. Bioleaching for Copper Extraction of Marginal Ores from the
668 Brazilian Amazon Region. Metals (Basel). 9, 81. doi:10.3390/met9010081

669 Nawab, J., Khan, S., Xiaoping, W., 2018. Ecological and health risk assessment of
670 potentially toxic elements in the major rivers of Pakistan: General population vs.
671 Fishermen. Chemosphere 202, 154–164. doi:10.1016/j.chemosphere.2018.03.082

672 Nel, A., 2005. Atmosphere: Enhanced: Air Pollution-Related Illness: Effects of Particles.
673 Science (80-.). 308, 804–806. doi:10.1126/science.1108752

674 Noble, T.L., Parbhakar-Fox, A., Berry, R.F., Lottermoser, B., 2017. Mineral Dust
675 Emissions at Metalliferous Mine Sites, in: Environmental Indicators in Metal Mining.

676 Springer International Publishing, Cham, pp. 281–306. doi:10.1007/978-3-319-42731-
677 7_16

678 Onder, M., Yigit, E., 2009. Assessment of respirable dust exposures in an opencast coal
679 mine. Environ. Monit. Assess. 152, 393–401. doi:10.1007/s10661-008-0324-4

680 Paluchamy, B., Mishra, D.P., Panigrahi, D.C., 2021. Airborne respirable dust in fully
681 mechanised underground metalliferous mines – Generation, health impacts and control
682 measures for cleaner production. J. Clean. Prod. 296, 126524.
683 doi:10.1016/j.jclepro.2021.126524

684 Pan, K., Wang, W.-X., 2012. Trace metal contamination in estuarine and coastal
685 environments in China. Sci. Total Environ. 421–422, 3–16.
686 doi:10.1016/j.scitotenv.2011.03.013

687 Pandey, B., Agrawal, M., Singh, S., 2014. Assessment of air pollution around coal mining
688 area: Emphasizing on spatial distributions, seasonal variations and heavy metals, using
689 cluster and principal component analysis. Atmos. Pollut. Res. 5, 79–86.
690 doi:10.5094/APR.2014.010

691 Pandey, J.K. 2012. Dust control practices in the Indian mining industry. In: 12th coal
692 operators' conference University of Wollongong & the Australasian Institute of Mining
693 and Metallurgy, pp 185–192.

694 Petavratzi, E., Kingman, S., Lowndes, I., 2005. Particulates from mining operations: A
695 review of sources, effects and regulations. Miner. Eng. 18, 1183–1199.
696 doi:10.1016/j.mineng.2005.06.017

697 Plumlee, G.S., Ziegler, T.L., 2007. The Medical Geochemistry of Dusts, Soils, and Other
698 Earth Materials, in: Treatise on Geochemistry. Elsevier, pp. 1–61. doi:10.1016/B0-08-
699 043751-6/09050-2

700 Querol, X., Alastuey, A., Rodríguez, S., Plana, F., Ruiz, C.R., Cots, N., Massagué, G.,
701 Puig, O., 2001. PM10 and PM2.5 source apportionment in the Barcelona Metropolitan

Area, Catalonia Spain. Atmos. Environ. 35, 6407–6419. Doi:10.1016/S1352-2310(01)00361-2

Reimann, C., de Caritat, P., 2005. Distinguishing between natural and anthropogenic sources for elements in the environment: regional geochemical surveys versus enrichment factors. Sci. Total Environ. 337, 91–107. doi:10.1016/j.scitotenv.2004.06.011

Rieuwerts, J.S., Mighanetara, K., Braungardt, C.B., Rollinson, G.K., Pirrie, D., Azizi, F., 2014. Geochemistry and mineralogy of arsenic in mine wastes and stream sediments in a historic metal mining area in the UK. Sci. Total Environ. 472, 226–234. doi:10.1016/j.scitotenv.2013.11.029

Rivera, M.B., Giráldez, M.I., Fernández-Caliani, J.C., 2016. Assessing the environmental availability of heavy metals in geogenically contaminated soils of the Sierra de Aracena Natural Park (SW Spain). Is there a health risk? Sci. Total Environ. 560–561, 254–265. doi:10.1016/j.scitotenv.2016.04.029

Romero-Baena, A.J., Barba-Brioso, C., Ross, A., González, I., Aparicio, P., 2021. Mobility of potentially toxic elements in family garden soils of the Riotinto mining area. Appl. Clay Sci. 203, 105999. doi:10.1016/j.clay.2021.105999

Romero, A., González, I., Martín, J.M., Vázquez, M.A., Ortiz, P., 2015. Risk assessment of particle dispersion and trace element contamination from mine-waste dumps. Environ. Geochem. Health 37, 273–286. doi:10.1007/s10653-014-9645-0

Sáez, R., Almodóvar, G.R., Pascual, E., 1996. Geological constraints on massive sulphide genesis in the Iberian Pyrite Belt. Ore Geol. Rev. 11, 429–451. doi:10.1016/S0169-1368(96)00012-1

Sánchez de la Campa, A.M., Sánchez-Rodas, D., Alsioufi, L., Alastuey, A., Querol, X., de la Rosa, J.D., 2018. Air quality trends in an industrialised area of SW Spain. J. Clean. Prod. 186, 465–474. doi:10.1016/j.jclepro.2018.03.122

727 Sánchez de la Campa, A.M., Sánchez-Rodas, D., Márquez, G., Romero, E., de la Rosa,
728 J.D., 2020. 2009–2017 trends of PM10 in the legendary Riotinto mining district of SW
729 Spain. Atmos. Res. 238, 104878. doi:10.1016/j.atmosres.2020.104878

730 Tornos, F., 2006. Environment of formation and styles of volcanogenic massive sulfides:
731 The Iberian Pyrite Belt. Ore Geol. Rev. 28, 259–307.
732 doi:10.1016/j.oregeorev.2004.12.005

733 Tóth, G., Hermann, T., Da Silva, M.R., Montanarella, L., 2016. Heavy metals in
734 agricultural soils of the European Union with implications for food safety. Environ. Int.
735 88, 299–309. doi:10.1016/j.envint.2015.12.017

736 UNE-EN 12341, 2015. Standard Gravimetric Measurement Method for Determination of
737 the PM10 or PM2.5 Mass Concentration of Suspended Particulate Matter.

738 Vega, M.A., Kulkarni, H. V., Johannesson, K.H., Taylor, R.J., Datta, S., 2020.
739 Mobilization of co-occurring trace elements (CTEs) in arsenic contaminated aquifers in
740 the Bengal basin. Appl. Geochemistry 122, 104709.
741 doi:10.1016/j.apgeochem.2020.104709

742 Viana, M., Kuhlbusch, T.A.J., Querol, X., Alastuey, A., Harrison, R.M., Hopke, P.K.,
743 Winiwarter, W., Vallius, M., Szidat, S., Prévôt, A.S.H., Hueglin, C., Bloemen, H.,
744 Wåhlin, P., Vecchi, R., Miranda, A.I., Kasper-Giebl, A., Maenhaut, W., Hitzenberger, R.,
745 2008. Source apportionment of particulate matter in Europe: A review of methods and
746 results. J. Aerosol Sci. 39, 827–849. doi:10.1016/j.jaerosci.2008.05.007

747 Wagner, A.C., Bergen, A., Brilke, S., Bühner, B., Ebert, M., Haunold, W., Heinritzi, M.,
748 Herzog, S., Jacobi, S., Kürten, A., Piel, F., Ramme, A., Weber, D., Weinbruch, S.,
749 Curtius, J., 2017. Characterization of Aerosol Particles Produced by a Skyscraper
750 Demolition by Blasting. J. Aerosol Sci. 112, 11–18. doi:10.1016/j.jaerosci.2017.06.007

751 Wei, X., Gao, B., Wang, P., Zhou, H., Lu, J., 2015. Pollution characteristics and health
752 risk assessment of heavy metals in street dusts from different functional areas in Beijing,
753 China. Ecotoxicol. Environ. Saf. 112, 186–192. doi:10.1016/j.ecoenv.2014.11.005

754 Williamson, K., Das, S., Ferro, A.R., Chellam, S., 2021. Elemental composition of indoor
755 and outdoor coarse particulate matter at an inner-city high school. Atmos. Environ. 261,
756 118559. doi:10.1016/j.atmosenv.2021.118559

757 World Health Organization 1999. Hazard Prevention and Control in the Work
758 Environment: Airborne Dust, World Health Organization, Switzerland,
759 WHO/SDE/OEH/99.14.

760 Zawadzka-Malota, I., 2015. Testing of mining explosives with regard to the content of
761 carbon oxides and nitrogen oxides in their detonation products. J. Sustain. Min. 14, 173–
762 178. doi:10.1016/j.jsm.2015.12.003

763 Zoller, W.H., Gladney, E.S., Duce, R.A., 1974. Atmospheric Concentrations and Sources
764 of Trace Metals at the South Pole. Science (80-.). 183, 198–200.
765 doi:10.1126/science.183.4121.198